Supplementary Material

Major Differences in Glycosylation and Fucosyltransferase Expression in Low-Grade Versus High-Grade Bladder Cancer Cell Lines

Bernadette Ezeabikwa[1,*], Nandini Mondal[2,*], Aristotelis Antonopoulos[3], Stuart M. Haslam[3], Yasuyuki Matsumoto[2], Miguel Martin-Caraballo[4], Sylvain Lehoux[2,5], Msano Mandalasi[1,6], Ali Ishaque[1], Jamie Heimburg-Molinaro[2], Richard D. Cummings[2,7] and Anthony K. Nyame[1,7]

[1]Department of Natural Sciences, University of Maryland Eastern Shore, Princess Anne, MD
[2]Department of Surgery, Beth Israel Deaconess Medical Center - Harvard Medical School, Boston, MA
[3]Department of Life Sciences, Imperial College London SW7 2AZ, UK
[4]Department of Pharmaceutical Sciences, School of Pharmacy, University of Maryland Eastern Shore, Princess Anne, MD
[5]Current address: Novab Inc., Atlanta, GA
[6]Current address: Department of Biochemistry and Molecular Biology, University of Georgia, Athens, GA

*These individuals should be considered as co-first authors

[7]Corresponding Authors:

Dr. Anthony Kwame Nyame
Department of Natural Sciences
University of Maryland Eastern Shore
Princess Anne, MD 21853
Tel: 1-410-603-8999
aknyame@gmail.com

Dr. Richard D. Cummings
Department of Surgery
Beth Israel Deaconess Medical Center
Harvard Medical School
CLS 11087 - 3 Blackfan Circle
Boston, MA 02115
Tel: 1-617-735-4643
rcummin1@bidmc.harvard.edu

Running title: Differential fucosylation in low- and high-grade bladder cancer

Keywords: Bladder cancer, Glycan marker, Lewis-X, Fucosyltransferase, Glycomics

Supplementary material information: This manuscript contains Supplementary Table I and Supplementary Figures 1-8

Supplementary Figure Legends

Supplementary Figure 1. **Immunofluorescence analysis of bladder cancer cell lines for the presence of Lewis antigens. (A)** RT4, J82COT, T24, TCCSUP and HL-60 control cells were incubated with anti-Le^x IgG mAb F8A1.1 and bound antibodies were detected by incubation with Alexa-488 conjugated goat anti-mouse IgG followed by fluorescence microscopy imaging. Panels **a** and **c**: phase contrast images, Panels **b** and **d**: fluorescence images; Panels **a** and **b**: control incubation conducted without mAb F8A1.1; Panels **c** and **d**: incubation conducted with mAb F8A1.1. **(B)** RT4, T24, and HL-60 control cells were incubated with anti-sialyl-Le^x IgM mAb HECA452 and bound antibodies were detected with Alexa-488 conjugated goat anti-rat IgM followed by imaging by fluorescence microscopy. Panels **a** and **c:** phase contrast images; Panels **b** and **d**: fluorescence images; Panels **a** and **b**: incubation with HECA452; Panels **c** and **d**: mock incubation lacking HECA452. **(C)** Western blot analysis of Le^x-bearing glycoproteins immunoprecipitated from extracts of J82COT, RT4, and T24 cells using mAb F8A1.1 (lanes indicated by +). Mock immunoprecipitations were carried out by omitting mAb F8A1.1 from the immunoprecipitation complex (lanes indicated by -).

Supplementary Figure 2 (related to Figure 2, panel A). Binding of HECA452 mAb to bladder cancer cells. (A) Flow cytometry histograms showing staining of (***left***) normal bladder epithelial cells A/T/N, (***middle***) low-grade bladder cancer cells RT4, and *(**right**)* high-grade bladder cancer cells T24 with either isotype control (open histograms) or mAb HECA452 (grey histograms). **(B)** Flow cytometry histograms showing staining of (***left***) low-grade bladder cancer cell line 5637 and (***right***) low-grade bladder cancer cell line SW780

with either isotype control (light grey histograms) or mAb HECA452 (dark grey histograms).

Supplementary Figure 3 (related to Figure 2, panel B). Expression of sialo-fucosylated lactosaminyl glycans by bladder cancer cells. Flow cytometry histograms showing staining of **(A)** normal bladder epithelial cells A/T/N, **(B)** low-grade bladder cancer cells RT4, and **(C)** high-grade bladder cancer cells T24 with plant lectins, *from left to right*, AAL, MAL-I, MAL-II, SNA, and PHA-L. Open histograms present staining with secondary detection reagent alone (Streptavidin-Alexa488) and grey histograms present staining with respective plant lectin. **(D)** Flow cytometry histograms showing staining of low-grade bladder cancer cell lines 5637 (***left***) and SW780 *(**right**)* with respectively from top to bottom, secondary detection reagent alone, AAL, MAL-I, MAL-II, and PHA-L lectins. **(E)** Flow cytometry histograms showing staining of low-grade bladder cancer cell lines 5637 (***left***) and SW780 *(**right**)* with secondary detection reagent alone *(**top histogram**)* and SNA lectin *(**bottom histogram**)*.

Supplementary Figure 4. **Immunofluorescence** a**nalysis to assess binding of plant lectins on the membrane of bladder cancer cells.** A/T/N, RT4, J82COT, T24, and TCCSUP cells were incubated with biotinylated lectins detected with Alexa-488-conjugated streptavidin. **(A)** AAL staining. +Fucose indicates addition of fucose to confirm lectin binding specificity. –AAL indicates streptavidin alone control. **(B)** L-PHA staining. +GalNAc indicates addition of GalNAc to confirm L-PHA binding specificity. For **A** and **B**, **Panels a, c, e:** phase contrast images, **Panels b, d, f:** fluorescence images. **(C)** Western blot analysis of lysates of A/T/N, RT4, J82COT, T24, and TCCSUP using AAL lectin as probe.

Identical amount of cell lysate protein was analyzed for each cell line. ***(Left panel)*** AAL blot of untreated cell lysates. –Fucose: free fucose was not added during blotting. +Fucose: free fucose was added during blotting to confirm AAL binding specificity. ***(Middle panel)*** AAL blot of cell lysates either untreated (-) or treated with PNGase F (+). ***(Right panel)*** AAL blot without (-NaOH) or with (+NaOH) β-elimination of O-glycans using NaOH.

Supplementary Figure 5. MALDI-TOF MS spectrum of permethylated N-glycans derived from **(A)** A/T/N, **(B)** T24, and **(C)** RT4 cell lines. Permethylated N-glycans were eluted at the 50% acetonitrile fraction (**Materials and Methods**). Main structures are depicted. Structures above a bracket have not had their location unequivocally defined. Putative structures are based on composition, tandem MS and knowledge of biosynthetic pathways. All molecular ions are $[M+Na]^+$.

Supplementary Figure 6. MALDI-TOF/TOF MS/MS spectra of the molecular ions at **(A)** m/z 3316 and **(B)** m/z 3490 selected from A/T/N cell lines (**Supplementary Figure 5A**). Structures outside a bracket have not had their location unequivocally defined. Putative structures are based on composition, tandem MS and knowledge of biosynthetic pathways. All molecular ions are $[M+Na]^+$. Horizontal blue dashed lines with arrowheads indicate the losses of the corresponding structures from the molecular ions. Fragment ion peaks in green colour correspond to losses of two LacNAc repeats having attached various fucose residues, from the molecular ion. In **(B)** fragment ion peak marked with an asterisk (*) corresponds to a contamination fragment ion from the molecular ion at m/z 3503.

Supplementary Figure 7. MALDI-TOF/TOF MS/MS spectra of the molecular ions at **(A)** m/z 5085, **(B)** m/z 5259, **(C)** m/z 5360, **(D)** m/z 5708, **(E)** m/z 5883 and **(F)** m/z 6332 selected from RT4 cell lines (**Supplementary Figure 5c**). Structures above/outside a bracket have not had their location unequivocally defined. Putative structures are based on composition, tandem MS and knowledge of biosynthetic pathways. All molecular ions are $[M+Na]^+$. Horizontal blue dashed lines with arrowheads indicate the losses of the corresponding structures from the molecular ions. Fragment ion peaks in green, yellow and red colours correspond to losses of two, three and four LacNAc repeats having attached various fucose residues, from the molecular ion respectively.

Supplementary Figure 8. Expression of fucosyltransferase genes in TCCSUP and J82COT cells. All gene expression is calculated using the ΔC_T method and expressed as per mille (‰) of GAPDH expression. (**A**) Bar plots present gene expression of FUTs 1-7. (**B**) Bar plots present gene expression of FUTs 8-11. Data are presented as Mean±SD of technical quadruplicates. Statistics: *t*-test was performed for each gene comparing the means of the two cell lines. Statistical significance was determined using Holm-Sidak method. $P<0.05$ is considered statistically significant difference. (**C**) Sequences of the primers used for gene expression analysis. All primer sequences were kindly provided by Dr. Kelley Moremen (Complex Carbohydrate Research Center, University of Georgia, Athens, Georgia).

Supplementary Table I

Supplemental Table 1. List of qRT-PCR primers used to amplify glycosyltransferase transcripts

Gene	Forward Primer (5'-3')	Reverse Primer (5'-3')	Source
FUT1	AGCAACGGCATGGAGTGGTGTA	AAGCCGAAGGTGCCAATGGTCA	Origene
FUT2	CTACCACCTGAACGACTGGATG	AGGGTGAACTCCTGGAGGATCT	Origene
FUT3	GCCGACCGCAAGGTGTAC	TGACTTAGGGTTGGACATGATATCC	(Higai *et al*, 2006)
FUT4	GGGTTTGGATGAACTTCGAGTCG	GGTAGCCATAAGGCACAAAGACG	(Mondal *et al*, 2018)
FUT5	ACCTGAGCTACTTTCACTGGCG	TCAGGTGAACCAAGCCGCTATG	(Mondal *et al*, 2018)
FUT6	CCGACTACATCACCGAGAAGCT	GAACCTCTCGTAGTTGCTTCTGC	(Mondal *et al*, 2018)
FUT7	GAATGAGAGCCGATACCAACGC	TAGCGGTCACAGATGGCACAGA	(Mondal *et al*, 2018)
FUT8	ATCCTGATGCCTCTGCAAAC	GGGTTGGTGAGCATAAATGG	(Bernardi, *et al* 2013)
FUT9	TCCCATGCAGTTCTGATCCAT	GAAGGGTGGCCTAGCTTGCT	(Higai *et al*, 2006)
FUT10	CTAACCAGCGACTTCTGACAGC	CCCATCTTTTGGGTGGTAAGCC	Origene
FUT11	ACACCTGGCTTTGGCAATGTGG	GTGGATCATGGCAGTGAGAGCT	Origene
ST3Gal I	AAGAGGACCCTGAAAGTGCTC	CTCCAGGACCATCTGCTTGG	(Silva *et al*, 2017)
ST3Gal3	GCCTGCTGAATTAGCCACCAA	GCCCACTTGCGAAAGGAGT	(Silva *et al*, 2017)
ST3Gal4	CTTCCTGCGGCTTGAGGATTA	CTCACTCCCCTTGGTCCCATA	(Silva *et al*, 2017)
ST3Gal6	ACTGCATTGCATATTATGGGGAA	TGGCTTTGATAAACAAGGCTGG	(Mondal et al., 2018)
ST6Gal I	CTGAATGGGAGGGTTATCTGCC	ACCTCAGGACTGCGTCATGATC	(Silva *et al*, 2017)
ST6Gal2	ACGCTGCTGATTGACTCTTCT	CACATACTGGCACTCATCTAA	(Ma *et al*, 2014)
ST6GALNACI	CTCTCTTCCTGGACTCCAGACA	AAGCGTGTCACGACCTTCTGCA	Origene
ST6GalNAcII	ACTTCCGTGGCCTGTTCAATC	GGCGATGACTTGGTGAGAGAG	(Silva *et al*, 2017)
ST6GALNAC3	TACGTGACCACAGAGAAGCGCA	CGTGAATGCCATAACAGGCGTC	Origene
ST6GALNAC5	GATTACTCGCCACAAGATGCTGC	GATCCTGTCACAGAGCTCCAGT	Origene
ST6GALNAC6	TGAGGTCTTCCATTACGGCTCC	CTGCTGACAATCACACACTGGTG	Origene
B4GalT1	GTATTTTGGAGGTGTCTCTGCTC	GGGCGAGATATAGACATGCCTC	(Mondal *et al*, 2018)
B4GalT2	GACCGCGACAAGCATAACGAAC	AGACACCTCCAAGACCTGGTAC	Origene
B4GalT3	TCCTCAAGGTCTGCCCTACTGT	ATTCCGCTCCACAATCTCTGCC	Origene
B4GalT4	CTCTGACTAATGAAGCATCCACG	CTGCCTGTACCTCTTCCAAAGTG	Origene
B4GalT5	GAAGATGACGACCTCTGGAACAG	GCCGTTCTTTTGACTTCCTCAGC	Origene
B4GalT6	CTCATTCCTTTCCGTAATCGCCA	GCCCACATTGAAAAGCATCGCAC	Origene
B4GalT7	TGCTCAACCAGGTGGACCACTT	AGGTCAACGTCGTGCATGGCAA	Origene
B3GALT1	CCTCATCAGCACCACTCACAAG	TGGCTCTCTTGCTCCACCATCT	Origene
B3GALT2	GTGTTCAATCACTGGCGAGTCTC	TTGCTGCGTTGGCACAGGCATT	Origene
B3GALT4	TCCTACCGCAACCTCACCCTAA	TCGCAAGACCAGCTCTGATACC	Origene
B3GALT5	AGCGGAAACGAAAGAGGTGGAC	CCTGAGGACAAAAGCGATGGAC	Origene
B3GALT6	ACCAGTACCTGGTGACGCACAA	GACCAGTCGTACACGTAGGACA	Origene
GCNT1	AACCCCTTAGTAAAGAAGAGGCG	AGCAGCCTGTCAAGCATTTCA	(Silva *et al*, 2017)
GCNT3-For	CACCAGAGACTGTGAGCACTTC	CATACACAGCTCGCAGTAGCCT	Origene
GCNT4-For	CTCTCCTGATGAGCACTTTTGGG	CCACTTGACAAGGCGAGTCTTAC	Origene
MGAT1	CCTATGACCGAGATTTCCTCGC	TGAAGCTGTCCCTGCCCGTATA	(Mondal *et al*, 2018)
GCNT2-For	TCCTGGTCCAAGGACACCTACA	CTGAGGTTTCCAGTCCAGGATG	Origene
GAPDH	CAGCCTCAAGATCATCAGC	ACAGTCTTCTGGGTGGCA	(Mondal *et al*, 2018)
B-Actin	CACCATTGGCAATGAGCGGTTC	AGGTCTTTGCGGATGTCCACGT	(Mondal *et al*, 2018)

References for Supplementary Table I

Bernardi, C., Soffientini, U., Piacente, F., & Tonetti, M. G. (2013). Effects of microRNAs on fucosyltransferase 8 (FUT8) expression in hepatocarcinoma cells. *PloS one, 8*(10), e76540-e76540. doi:10.1371/journal.pone.0076540

Higai, K., Ishihara, S., & Matsumoto, K. (2006). NFκB-p65 Dependent Transcriptional Regulation of Glycosyltransferases in Human Colon Adenocarcinoma HT-29 by Stimulation with Tumor Necrosis Factor &alpha. *Biological and Pharmaceutical Bulletin, 29*(12), 2372-2377. doi:10.1248/bpb.29.2372

Mondal, N., Dykstra, B., Lee, J., Ashline, D. J., Reinhold, V. N., Rossi, D. J., & Sackstein, R. (2018). Distinct human α(1,3)-fucosyltransferases drive Lewis-X/sialyl Lewis-X assembly in human cells. *Journal of Biological Chemistry, 293*(19), 7300-7314. doi:10.1074/jbc.RA117.000775

Silva, M., Fung, R. K. F., Donnelly, C. B., Videira, P. A., & Sackstein, R. (2017). Cell-Specific Variation in E-Selectin Ligand Expression among Human Peripheral Blood Mononuclear Cells: Implications for Immunosurveillance and Pathobiology. *Journal of immunology (Baltimore, Md. : 1950), 198*(9), 3576-3587. doi:10.4049/jimmunol.1601636

Supplementary figure 1

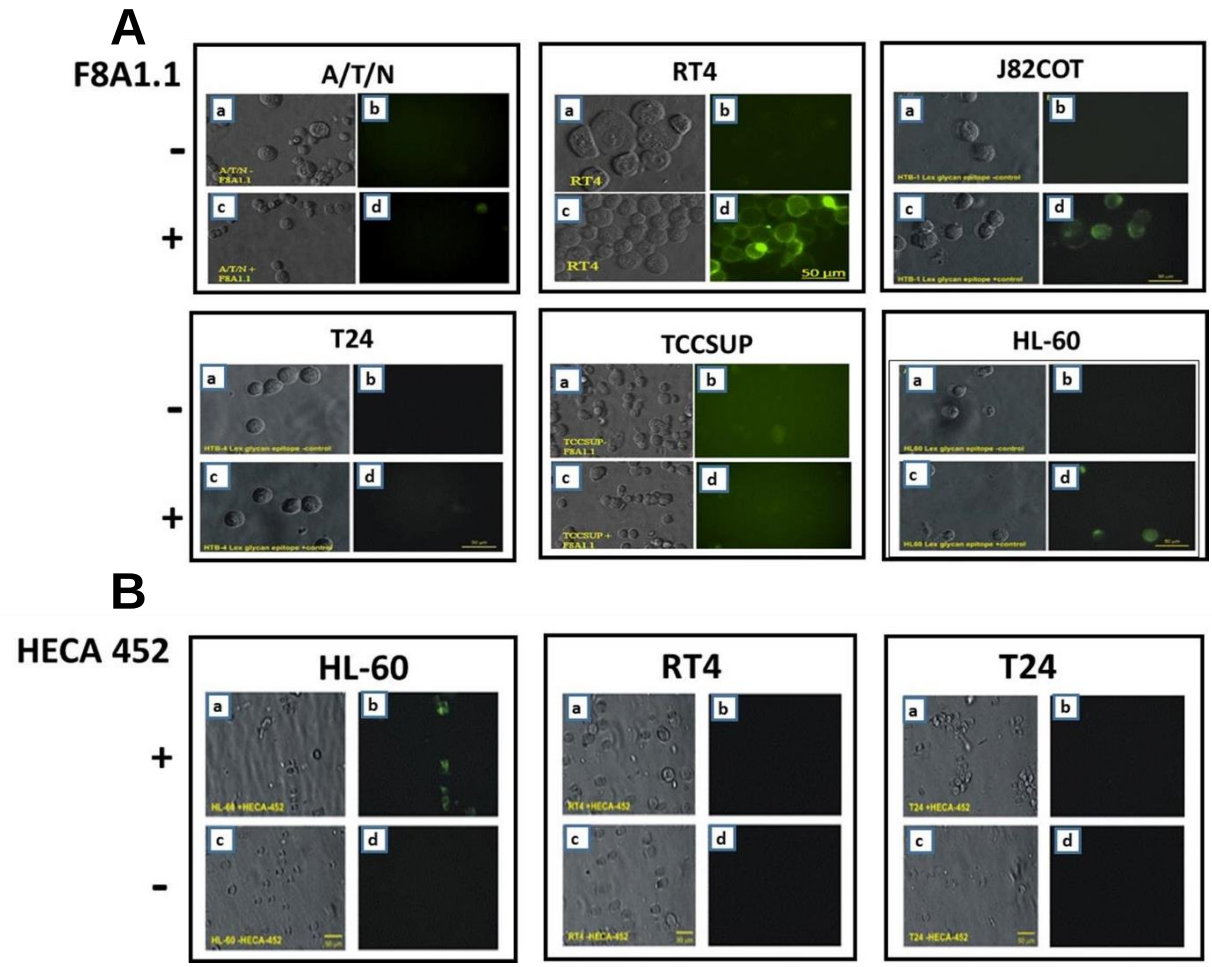

Supplementary figure 2

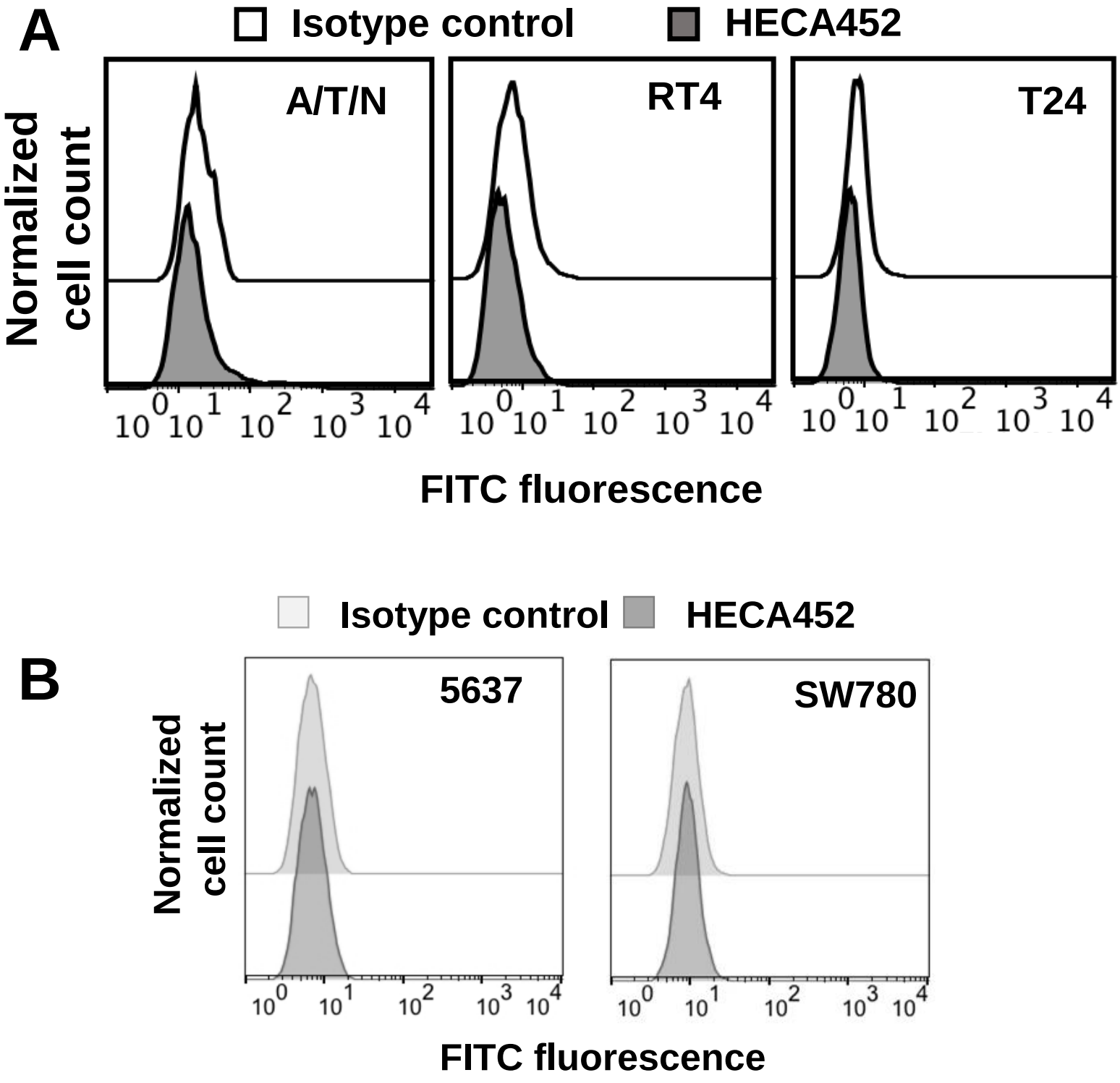

Supplementary figure 3

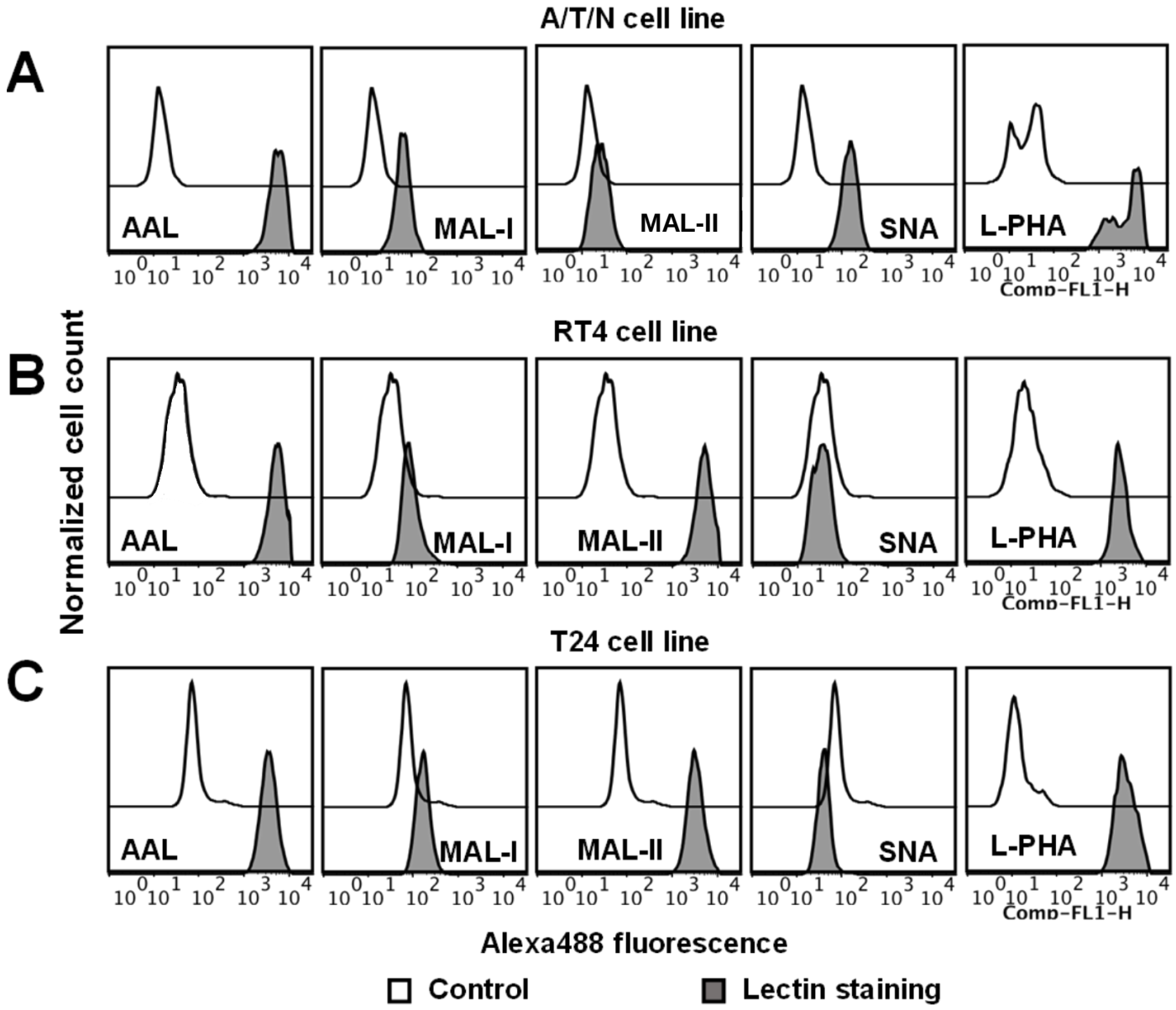

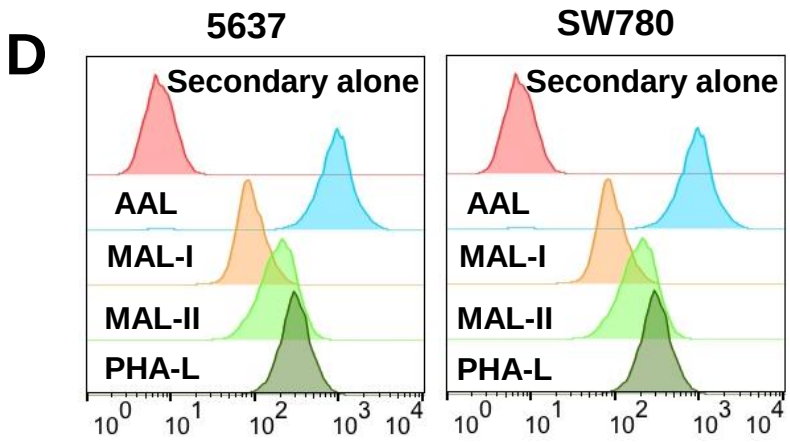

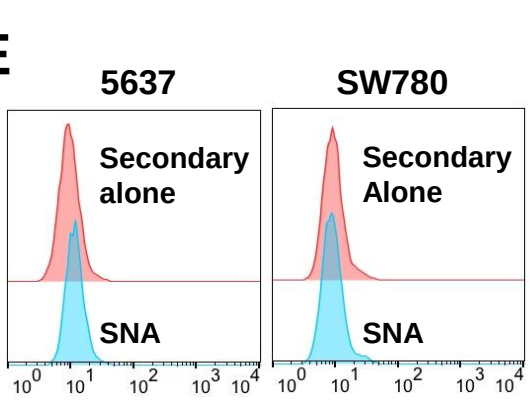

Supplementary figure 4

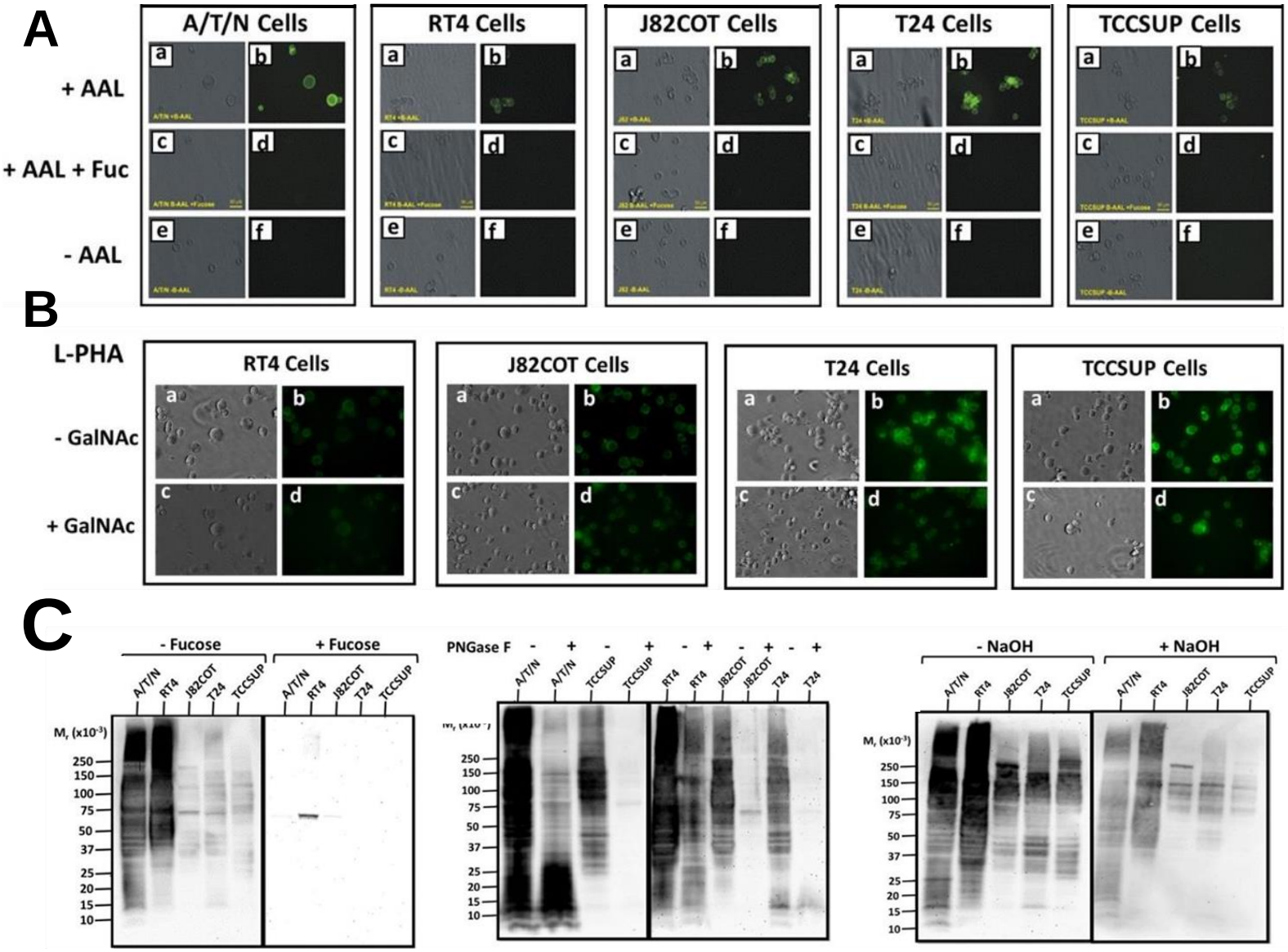

Supplementary figure 5

5A

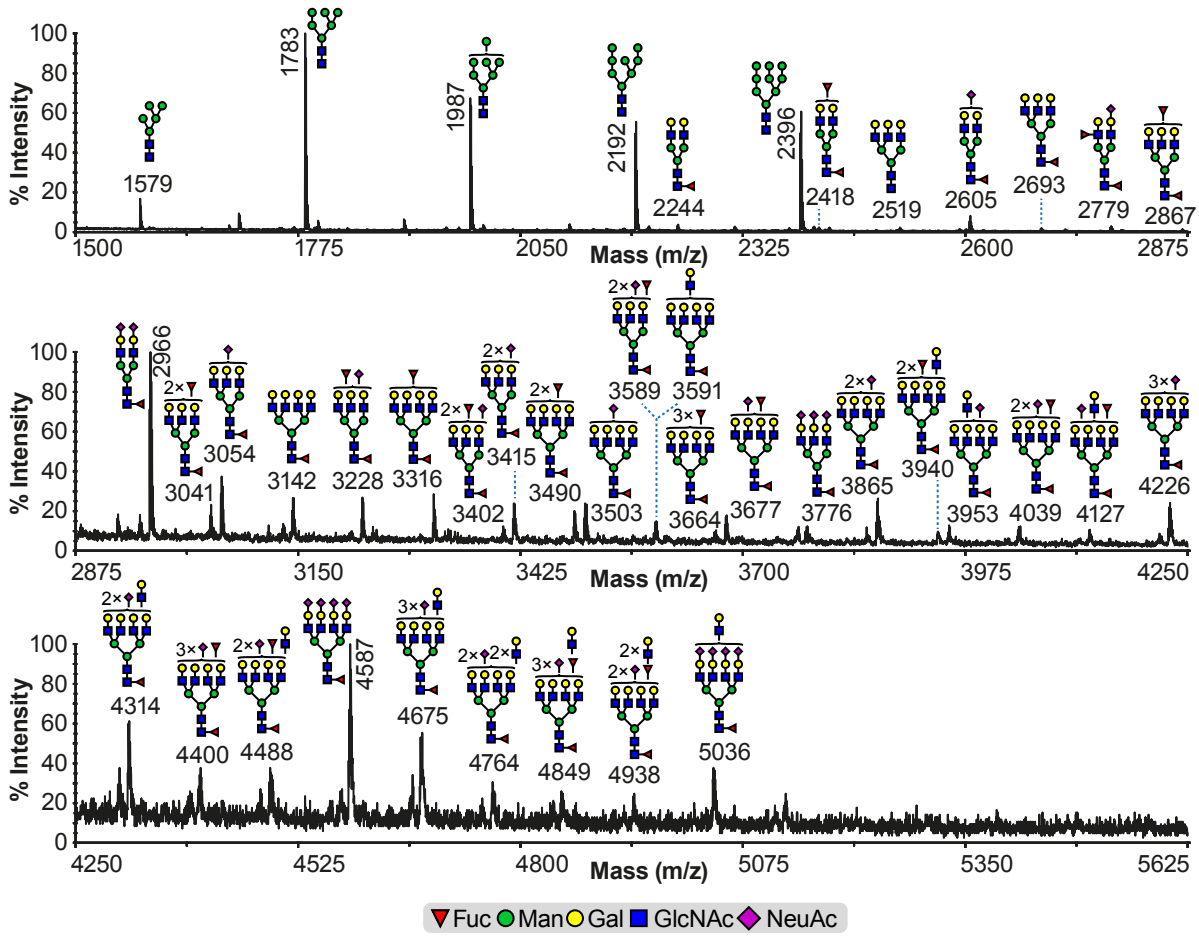

Supplementary figure 5

5B

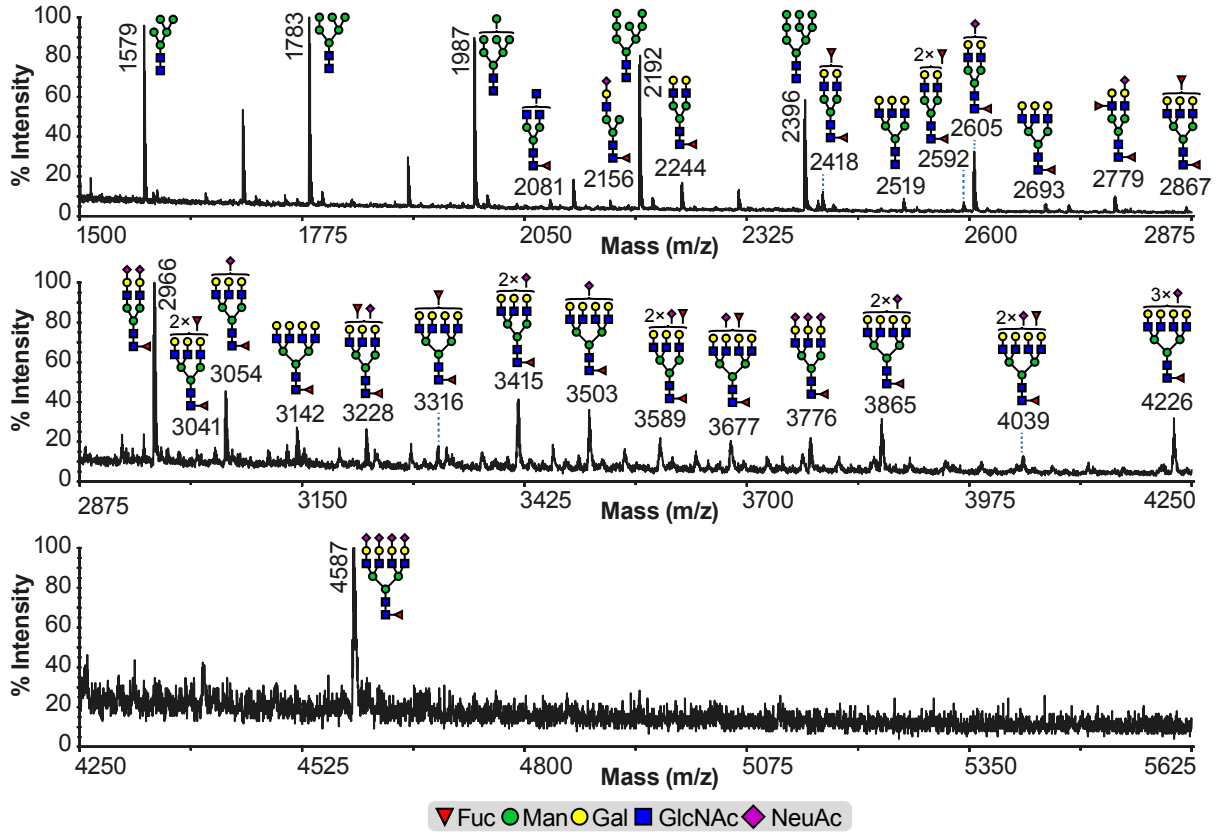

Supplementary figure 5

5C

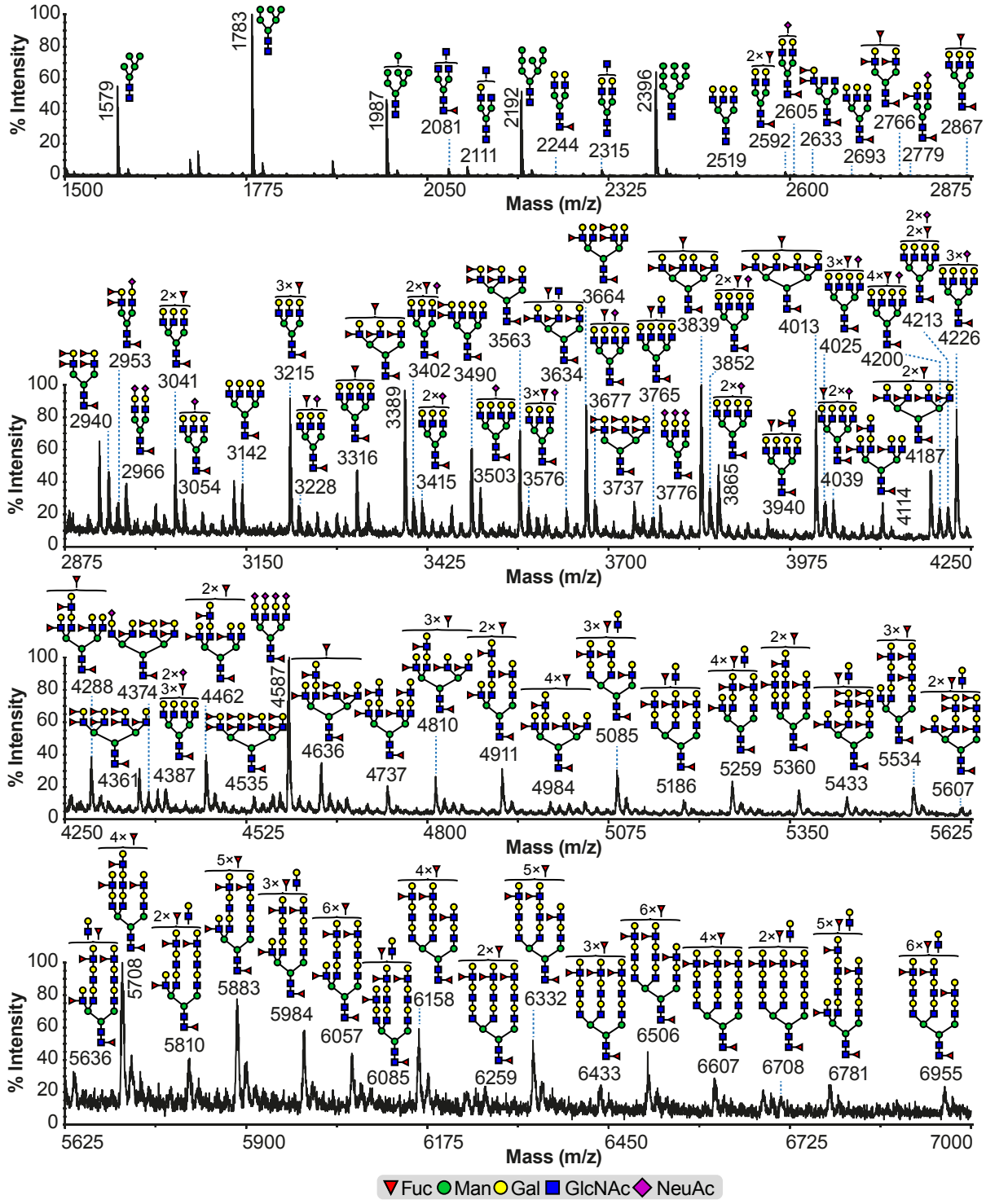

Supplementary figure 6

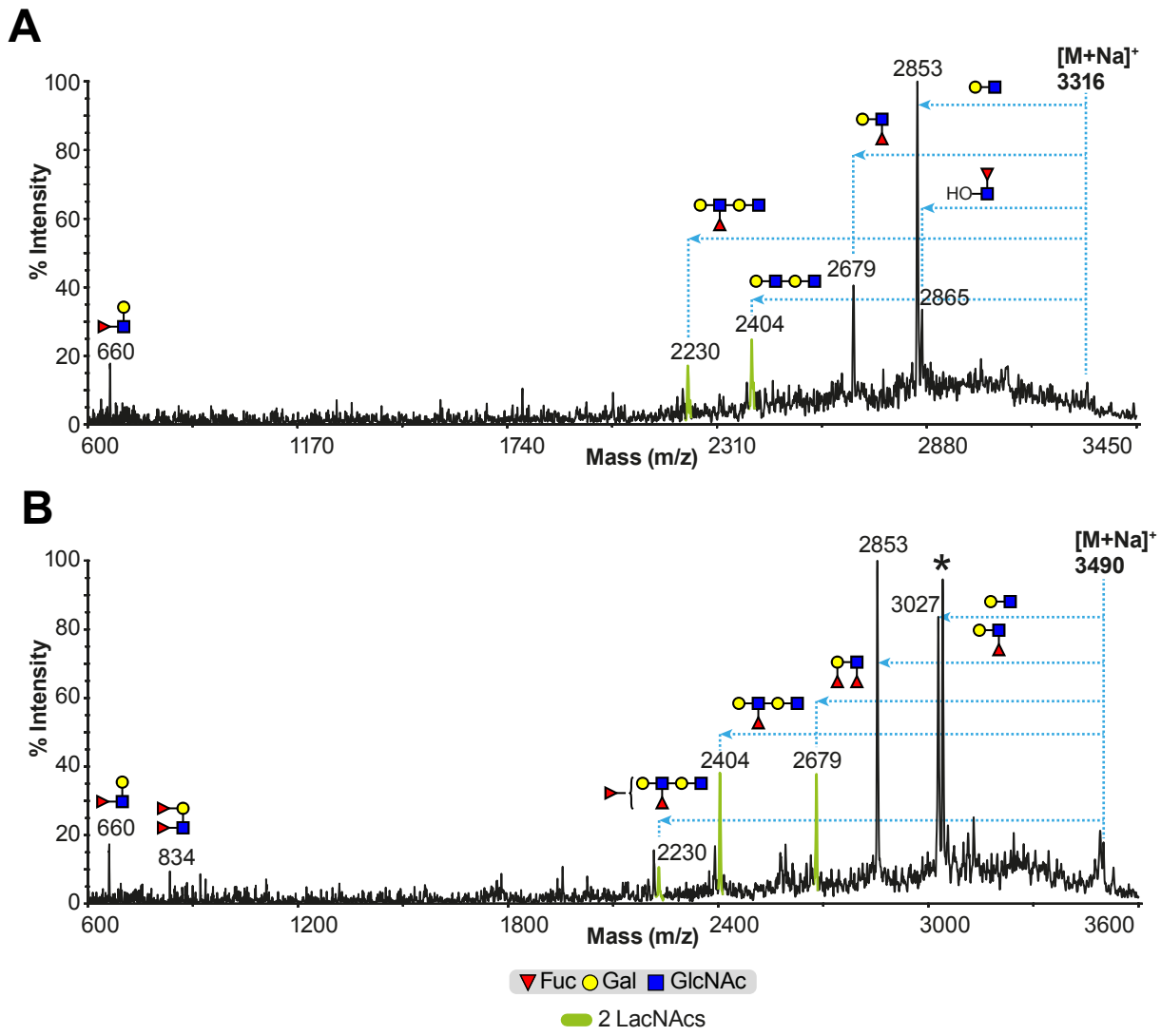

Supplementary figure 7

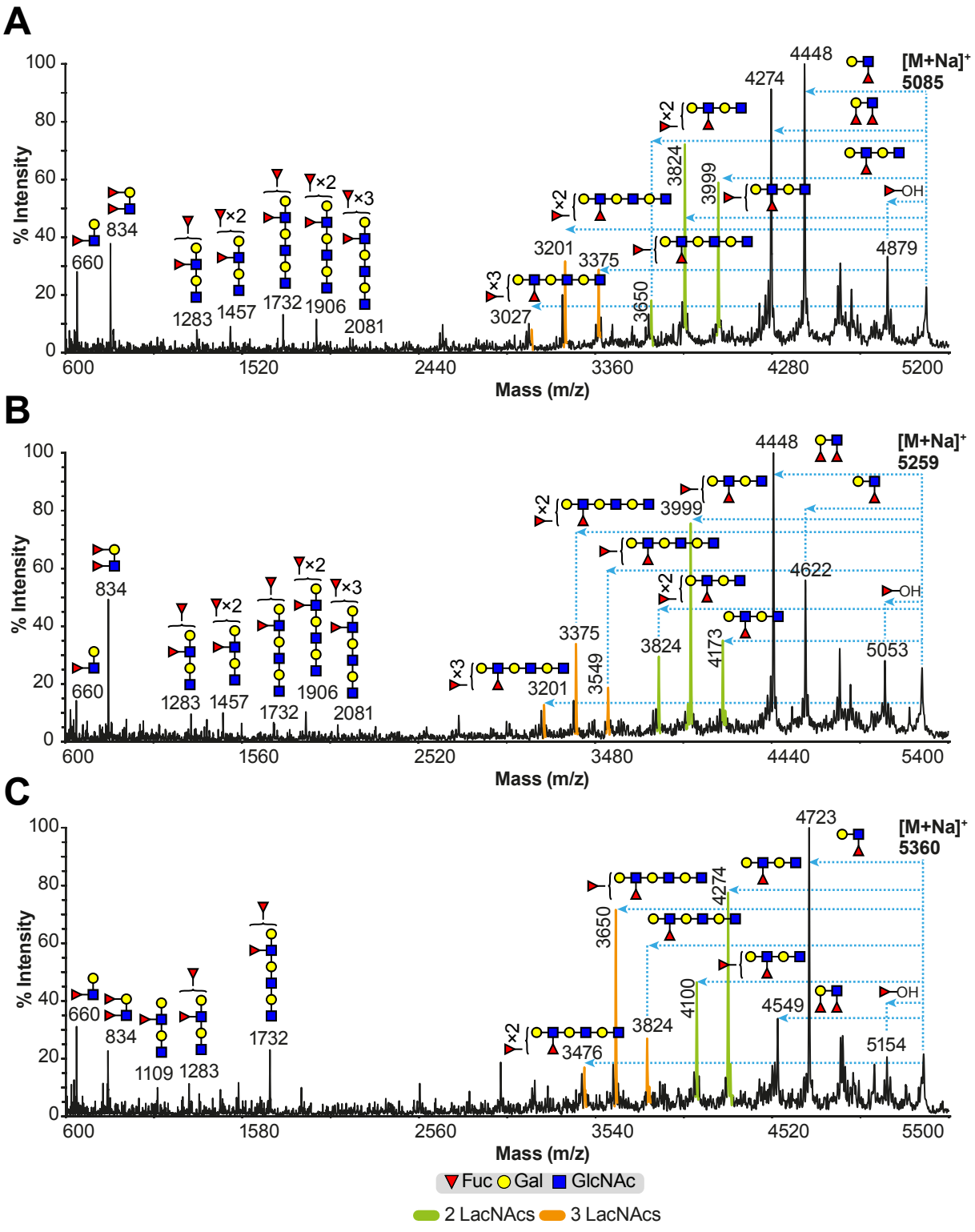

Supplementary figure 7

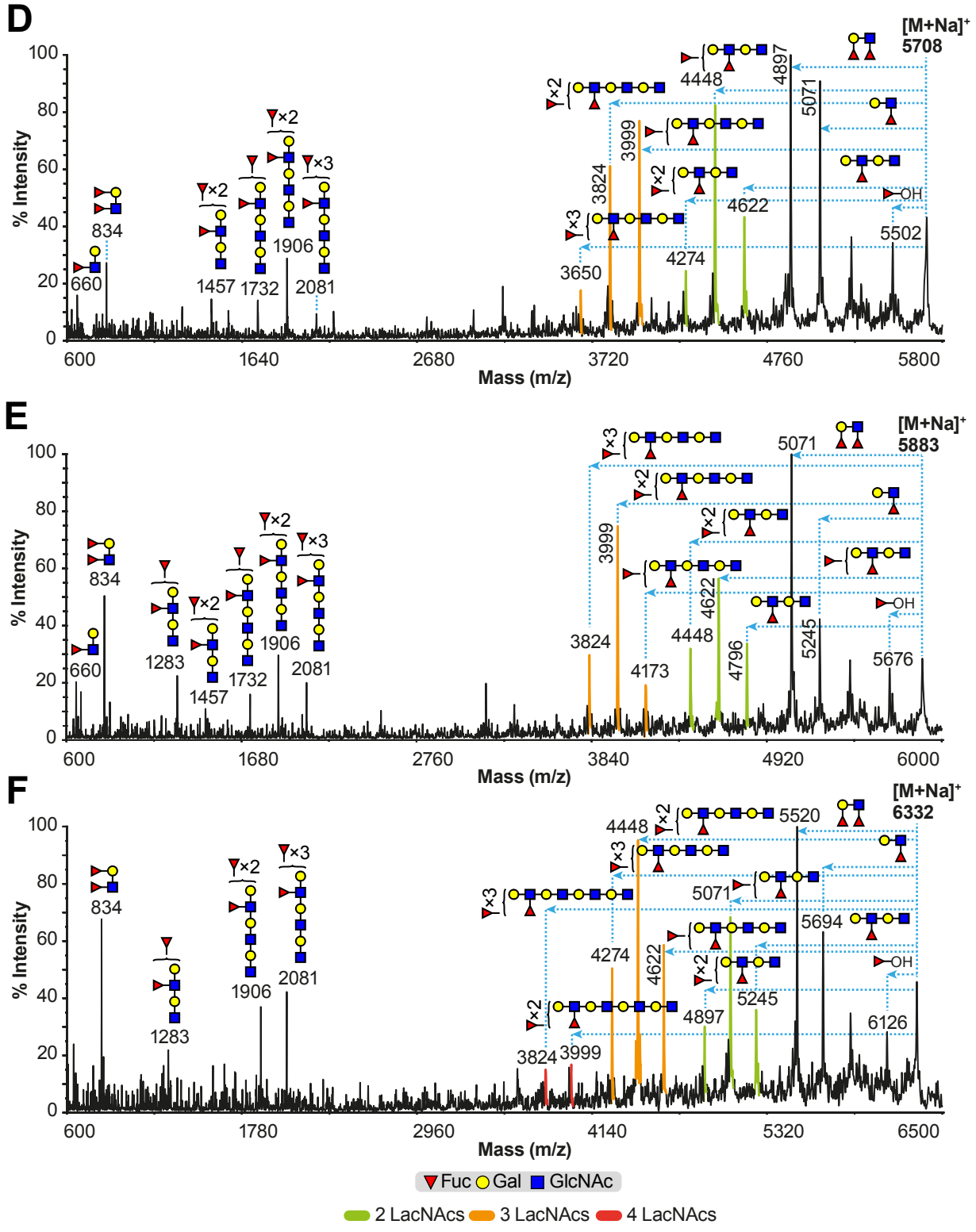

Supplementary figure 8

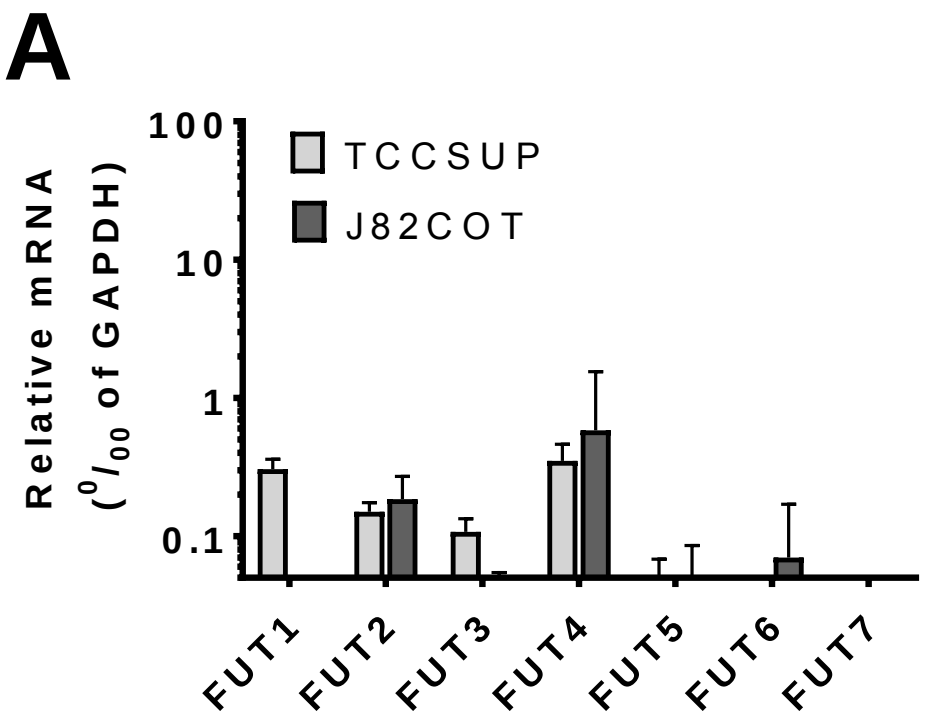

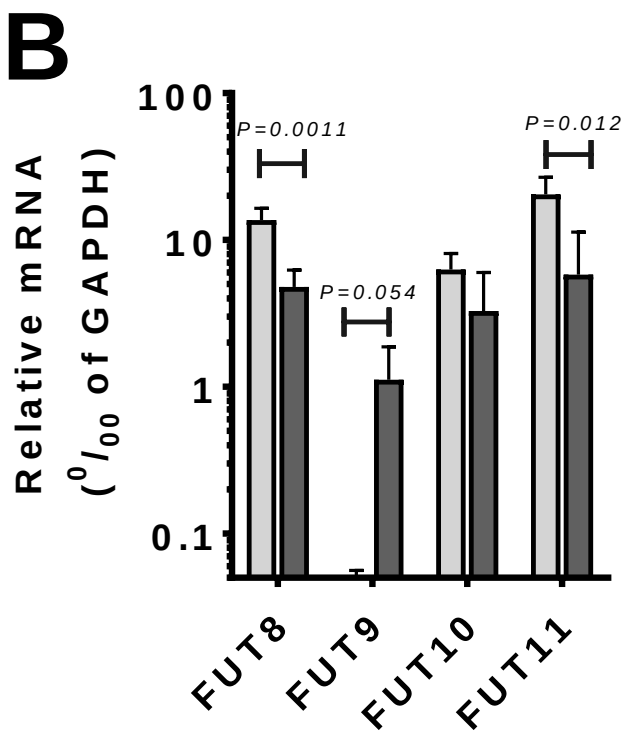

C

Gene	Forward Primer (5'-3')	Reverse Primer (5'-3')
FUT1	GGCCTTCCTGCTAGTCTGTG	GCCATGTGGAAAGCTGTCTT
FUT2	GATTCAAGCCATGTGGGAGT	GTCCCAGTGCCTTTGATGTT
FUT3	CGCTGGATCTGGTTCAACTT	GTATCTGTCCAGGGCTTCCA
FUT4	TGGCCCGCTACAAGTTCTAC	GCCAGAGCTTCTCGGTGATA
FUT5	ACATCACTGCCGACTCCAGT	CATGATATCCCAGTGGTGCA
FUT6	CTGCTGATGGCTGTGTGTTT	GGGTACACAGTGGGATCGTC
FUT7	GTGCATGTGGATGACTTTGG	GCTCTCATTCATGCCAGTGA
FUT8	GGTCGAGCTTCCCATTGTAG	GCGAGGTCTTCTGGTACAGC
FUT9	CTTACCGCCGTGATTCAGAT	AAACACGAAGGGATTTGTGC
FUT10	TATGTTCGCGAGCTGATGAC	TGAGGGAGGTCTTTGTTTCG
FUT11	AGTCTGAAGCATCGGGAGTG	TCGAAGCCGTTGAGGTAGTT